https://doi.org/10.5194/bg-2020-466
Preprint. Discussion started: 1 February 2021

Biogeosciences Discussions
Open Access
EGU

Mercury mobility, colloid formation and methylation in a polluted fluvisol as affected by manure application and flooding-draining cycle.

Lorenz Gfeller[1], Andrea Weber[1], Isabelle Worms[2], Vera I. Slaveykova[2], Adrien Mestrot[1]

[1]Institute of Geography, University of Bern, Hallerstrasse 12, 3012 Bern, Switzerland
[2]Environmental Biogeochemistry and Ecotoxicology, Department F.-A. Forel for environmental and aquatic sciences, School of Earth and Environmental Sciences, Faculty of Sciences, University of Geneva, Uni Carl Vogt, Bvd Carl-Vogt 66, CH-1211 Geneva 4, Switzerland
Correspondence to: Adrien Mestrot (adrien.mestrot@giub.unibe.ch)

https://doi.org/10.5194/bg-2020-466
Preprint. Discussion started: 1 February 2021

Biogeosciences Discussions Open Access EGU

Abstract

Floodplain soils polluted with high levels of mercury (Hg) are potential point sources to downstream eco-systems. Repeated flooding (e.g. redox cycling) and agricultural activities (e.g. organic matter addition) may influence the fate and speciation of Hg in these soil systems. The formation and aggregation of colloids and particles influences both Hg mobility and its bioavailability to methylmercury (MeHg) forming microbes. In this study, we conducted a microcosm flooding-draining experiment on Hg polluted floodplain soils originating from an agriculturally used area situated in the Rhone Valley (Valais, Switzerland). The experiment comprised two 14 days flooding periods separated by one 14 days draining period. The effect of freshly added natural organic matter on Hg dynamics was assessed by adding liquid cow manure (+MNR) to two control soils characterized by different Hg (47.3 ± 0.6 mg kg^{-1} or 2.38 ± 0.01 mg kg^{-1}) and organic carbon (OC: 1.92 wt. % or 3.45 wt. %) contents. During the experiment, the release, colloid formation and methylation of Hg in the soil solution were monitored. Upon manure addition in the highly polluted soil (lowest OC), an accelerated release of Hg to the soil solution could be linked to a fast reductive dissolution of Mn oxides. The manure treatments showed a fast sequestration of Hg and a higher percentage of particulate (0.02 – 10 µm) bound Hg. As well, analyses of soil solutions by asymmetrical flow field-flow fractionation coupled with inductively coupled plasma mass spectrometry (AF4–ICP–MS) revealed a proportional increase of colloidal DOM-Hg and inorganic colloidal Hg (+MNR: 70 - 100 %; control: 32 – 70 %) upon manure addition. Our experiment shows that net Hg methylation (MeHg/Hg) was highest after the first draining period and decreased again after the second flooding period. No significant effects on methylation upon manure addition was found. The results of this study suggest that manure addition may promote sequestration by Hg complexation on large organic matter components and the formation/aggregation of inorganic $HgS_{(s)}$ colloids in Hg polluted fluvisols with low levels of natural organic matter.

https://doi.org/10.5194/bg-2020-466
Preprint. Discussion started: 1 February 2021


Biogeosciences Discussions Open Access EGU

33

34 **1. Introduction**

35 Mercury (Hg) is a pollutant of global concern due to its high toxicity and to its global biogeochemical cycle which
36 spans all environmental compartments (atmosphere, oceans, soils etc.) (Beckers and Rinklebe, 2017; AMAP/UN
37 Environment, 2019). Sediments and soils are major Hg pools with relatively long residence times (Amos et al.,
38 2013; Driscoll et al., 2013). Legacy Hg from industrial sites (e.g. chloralkali plants or mining areas) retained in soils
39 are a key source for present day atmospheric Hg (Amos et al., 2013). However, this retained Hg pool can also be
40 remobilized by landscape alteration, land use (e.g. fertilization, manure addition) or climate induced changes such as
41 drought-flood-drought cycles of soils (Singer et al., 2016). These inputs are a threat to downstream ecosystems and
42 human health due to release of inorganic Hg and the formation and bioaccumulation of toxic monomethylmercury
43 (MeHg) in both aquatic and terrestrial food chains (Bigham et al., 2017).
44 Mercury is redox sensitive and occurs mainly as elemental Hg^0, inorganic Hg^{2+} or in the form of MeHg in soils. In
45 general, Hg speciation in soils depends on the biogeochemical conditions. For example, in natural organic matter
46 (NOM) rich boreal peatlands and forest soils, Hg is primarily bound to thiol-groups of NOM (NOM–Hg), or found
47 as $FeS_{(s)}$ or as cinnabar $HgS_{(s)}$, These species are the thermodynamically most favored forms of Hg in these envi-
48 ronments (Skyllberg et al., 2006; Skyllberg and Drott, 2010; Biester et al., 2002). However, Hg sorbed on the sur-
49 faces of manganese (Mn), iron (Fe) and aluminum (Al) oxy-hydroxides may also represent important Hg-pools in
50 soils with low amounts of NOM (Guedron et al., 2009).
51 The fate of Hg in soils is still not well characterized, and its mobilization and sequestration in soil depends on a
52 variety of factors and mechanisms. The release of Hg to the soil solution and its further transport has been associated
53 with the mobilization of NOM (Kronberg et al., 2016; Eklöf et al., 2018; Åkerblom et al., 2008), copper (Cu) nano-
54 particles (Hofacker et al., 2013) or the reductive dissolution of Fe/Mn-oxyhydroxides (Frohne et al., 2012; Gygax et
55 al., 2019; Poulin et al., 2016). Earlier studies reported an immediate decrease of dissolved Hg after its release upon
56 flooding in various riparian settings (Hofacker et al., 2013; Poulin et al., 2016; Gygax et al., 2019). Possible path-
57 ways for this decrease are Hg^{2+} reduction to Hg^0, sorption to recalcitrant NOM, formation of meta-cinnabar ß-$HgS_{(s)}$
58 or co-precipitation of Hg in sulfides (e.g. $FeS_{(s)}$) or metallic particles.
59 Metallic colloids in soil may be formed by e.g. biomineralization during soil reduction or precipitation in the root
60 zone and potentially incorporate toxic trace elements like Hg (Weber et al., 2009; Manceau et al., 2008). These
61 colloids may increase the mobility and persistence of toxic trace metals in soil solution if they do not aggregate to
62 bigger particles. During a flooding incubation experiment, Hofacker et al. 2013 observed the incorporation of Hg in
63 Cu nano-particles formed by biomineralization (Hofacker et al., 2015). Colloidal ß-$HgS_{(s)}$ has been reported to form
64 abiotically in soils under oxic conditions directly by interaction with thiol-groups of NOM (Manceau et al., 2015). In
65 solution, Dissolved Organic Matter (DOM) has a major influence in the formation and aggregation of metallic col-
66 loids and particles. It may promote the dissolution of $HgS_{(s)}$ (Miller et al., 2007) or decelerate the aggregation and
67 growth of Hg incorporating metal sulfide colloids by complexing Hg ions as well as altering the reaction kinetics of
68 e.g. $HgS_{(s)}$ formation. The same effect was also observed for other metal sulfide-, oxide- or carbonate colloids

https://doi.org/10.5194/bg-2020-466
Preprint. Discussion started: 1 February 2021

(Aiken et al., 2011). In case of Hg, this may in turn increase its mobility and bioavailability to MeHg producing microorganisms (Deonarine and Hsu-Kim, 2009; Ravichandran et al., 1999; Aiken et al., 2011; Graham et al., 2012). Chelation of Hg with larger NOM molecules may as well inhibit the microbial availability of Hg (Bravo et al., 2017). Within Hg–NOM, the sorption on larger thiol rich NOM is thermodynamically favored. However, different ligand exchange reactions (e.g. carboxyl-groups to thiol groups) kinetically control this sorption and thus the bioavailability of dissolved Hg in aqueous systems (Miller et al., 2007; Miller et al., 2009; Liang et al., 2019). The partly contradicting statements above illustrate the complex role of NOM and DOM on the Hg cycle and Hg bioavailability and the need for more research in this field.

The formation of MeHg from inorganic Hg^{2+} has been shown to be primarily microbially driven. Environments of redox oscillation (e.g. floodplains, estuaries) represent hot spots for Hg methylation (Marvin-DiPasquale et al., 2014; Bigham et al., 2017). Mercury methylators are usually anaerobe microbial species such as sulfate reducers (SRB), Fe reducers (FeRB), archaea and some firmicutes (Gilmour et al., 2013). Generally, Hg is bioavailable to methylators in the form of dissolved Hg^{2+}, Hg complexed by labile DOM, Hg bearing inorganic nanoparticles (e.g. $FeS_{(s)}$, $HgS_{(s)}$) but is less available when complexed by particulate organic matter (Hg–POM) or larger inorganic particles (Chiasson-Gould et al., 2014; Graham et al., 2013; Rivera et al., 2019; Zhang et al., 2012; Jonsson et al., 2012). Further, DOM is a main driver of Hg methylation as it influences both bioavailability and microbial activity. The role of DOM as electron donor may enhance the microbial activity and thus the cellular uptake. The composition and origin of DOM were reported to change Hg methylation rates (Drott et al., 2007; Bravo et al., 2017). For example, (Bravo et al., 2017) showed that in lake sediments, terrestrial derived DOM led to slower methylation rates than phytoplankton derived DOM. The addition of DOM in form of organic amendments (e.g. manure or rice straw) had been reported to have both an enhancing (Gygax et al., 2019; Liu et al., 2016; Wang et al., 2019) or no effect (Zhu et al., 2016; Liu et al., 2016) on the net-methylation in soils. Further, organic amendments were reported to shift microbial communities. Both the enhancement of Hg demethylators, Hg reducers (Hu et al., 2019) as well as the enhancement Hg methylators upon organic amendments were reported (Tang et al., 2019). Methylation hotspots (redox boundaries) are also places of NOM degradation and mineralization. The degradation of large NOM to more bioavailable low molecular weight (LMW) compounds promoted by microbial Mn oxidation, especially in systems with neutral pH (Jones et al., 2018; Sunda and Kieber, 1994; Ma et al., 2020), is also hypothesized to increase bioavailability of Hg–NOM. However, amendments of Mn oxides were also shown to inhibit Fe, SO_4^- reducing conditions and thus MeHg formation in sediments (Vlassopoulos et al., 2018).

Hg methylation and mobilization is intensively studied in paddy field soils and peat soils due to their relevance in food production or the Hg global cycle (Wang et al., 2019; Tang et al., 2018; Liu et al., 2016; Hu et al., 2019; Wang et al., 2016; Zhao et al., 2018; Zhu et al., 2016; Kronberg et al., 2016; Skyllberg, 2008; Skyllberg et al., 2006). However, only few studies focused on Hg methylation and mobility in temperate floodplain soils (Frohne et al., 2012; Hofacker et al., 2013; Weber et al., 2009; Gilli et al., 2018; Poulin et al., 2016). As well, few studies have examined the effect of flooding and/or land use (NOM addition in the form of animal manure) in polluted soils with respect to Hg release and methylation potential (Tang et al., 2018; Gygax et al., 2019; Zhang et al., 2018; Hofacker et al., 2013; Frohne et al., 2012). Furthermore, most of these studies were focusing on soils with rather high OC

https://doi.org/10.5194/bg-2020-466
Preprint. Discussion started: 1 February 2021

levels (5 – 10 wt. %) and only few researches have addressed the decrease of Hg in soil solution of flooded soils over time, including the fate of colloidal Hg.

This work focused on the effect of the agricultural practices on the Hg biogeochemistry in a contaminated fluvisol with specific emphasis on the flooding-draining cycle and manure addition. We studied the effect of these cycles and manure addition on 1.) the release and sequestration of Hg, 2.) the net-methylation of Hg and 3.) the evolution of colloidal and particulate Hg in soil solution. The latter was studied by analyzing different soil solution filter fractions (0.02/10 µm) as well as analyzing selected samples by asymmetric flow field flow fractionation coupled to a UV_{vis} detector, a fluorescence detector and an ICP–MS (AF4–ICP–MS).

2. Methods and Materials

2.1. Sample collection

We sampled soil from agriculturally used fields in the alpine Rhone Valley in Wallis, Switzerland on September 30th, 2019. The fields are situated in a former floodplain next to the artificial "Grossgrundkanal" canal. This canal was built in the 1900s to drain the floodplain and as a buffer for the emissions of an acetaldehyde producing chemical plant upstream. The soils on the floodplain were subjected to Hg pollution from this plant between the 1930s and the 1970s, mostly through the removal and dispersion of the canal sediments onto the agricultural fields (Glenz and Escher, 2011). After heavy rain events, the fields are subjected to draining-flooding cycles (Fig. S1) and have been identified as potential hotspots for Hg methylation and release (Gygax et al., 2019). For this study, soil was sampled from a cornfield and a pasture field next to the canal. A map and the coordinates of the sampling locations is provided in the supplement (Fig. S1, Table S1). At each site, a composite sample of approx. 10 kg of soil was sampled between 0 – 20 cm depth from ten points on the fields. The soil samples were named after their relative pollution and organic carbon levels (High Mercury, Low Carbon (HMLC) and Low Mercury, High Carbon (LMHC), see Part 4.3 below for details on the soils. After sampling, roots were removed, and the fresh soil was sieved to < 2 mm grain size, further homogenized, split in two parts and stored on ice in airtight PE Bags for transport to the laboratory. Additionally, approx. 2 L of liquid cow manure was sampled from a close-by cattle farm. One aliquot of the samples was stored at - 20° C until further processing. The remaining part was used for the incubation experiment within 12 h after sampling. A detailed description of the site and sampling procedures is given in the supplement (Sect. S1).

2.2 Incubation experimental setup.

An initial incubation was conducted in 10 L HDPE containers in the dark for seven days in an atmosphere of 22 °C and 60 % relative humidity (RH) in order to equilibrate the soils and to prevent a peak of microbial respiration induced by the soil sieving before the onset of the experiment (Fig. 1). After this initial incubation the soils were passed to the flooding-draining experiment. This was conducted in 1 L Borosilicate aspirator bottles. The environment created though soil flooding in these bottles will be called microcosm (MC) in the following text. The experiments were run in triplicates and named after the relative pollution and organic carbon levels of the used soil (HMLC and LMHC) and the treatment with or without manure addition (control and +MNR). The MCs were

https://doi.org/10.5194/bg-2020-466
Preprint. Discussion started: 1 February 2021

equipped with an acid washed suction cup with a pore size of < 10 µm (model: 4313.7/ETH, ecoTech Umwelt-Meßsysteme GmbH, Bonn, Germany). In the following sequence, 700 g of artificial rainwater (NH_4NO_3 11.6 mg L^{-1}/ K_2SO_4 7.85 mg L^{-1}/ Na_2SO_4 1.11 mg L^{-1}/ $MgSO_4 \cdot 7H_2O$ 1.31 mg L^{-1}/ $CaCl_2$ 4.32 mg L^{-1}) were added to the MCs. For the manure treatment, 0.6 % (w/w) (3 g) of liquid cow manure was added to the MCs corresponding to one application of liquid manure on a cornfield following the principles of fertilization of agricultural crops in Switzerland (Richner and Sinaj, 2017) and finally fresh soil was added with a $soil_{dry}$:water ratio of 1:1.4 (w/w) (Fig. S2). Then, the MCs were gently shaken for at least one minute to avoid any remaining air bubbles in the soil pore space. An additional mixture of fresh soil artificial rainwater (1:1.4 (w/w)) was shaken for 6 h to assess the equilibration of the solid and liquid phase during the experiment. The MCs were covered with Parafilm®, transferred to the incubation chamber (APT.line™ KBWF, Binder, Tuttlingen, Germany) and incubated in the dark for 14 days in atmosphere of 22 °C and 60 % RH. The incubation temperature was chosen to be close to the daily mean soil temperature in 10 cm depth during summer months between 2015–2019 (21.4 °C) at the closest soil temperature monitoring station (Sion, VS, provided by MeteoSwiss) situated downstream. After the first flooding period, the supernatant water was pipetted off, and remaining water was sampled through the suction cups to drain the MCs. They were weighted before and after water removal. Then, approximately 25 g of moist soil was sampled by two to three scoops though the whole soils column using a disposable lab spoon. The MCs were kept drained in an atmosphere of 22 °C and 10 % RH for 14 days. For the second flooding period, the incubators were again flooded with 500 g of artificial rainwater and incubated for another 14 days in an atmosphere of 22 °C and 60 % RH (Fig. 1). After the incubation, the suction cups were removed, the soils were homogenized and then transferred from the MC to a PE bag and stored at -20 °C until further processing.

2.3 Soil and manure characterization

Frozen soil and manure samples were freeze dried to avoid a loss of Hg prior to analyses (Hojdová et al., 2015), ground using an automatic ball mill (MM400, Retsch, Haan, Germany) and analyzed for the following chemical parameters. Carbon (C), nitrogen (N) and sulfur (S) were measured with an elemental analyzer (vario EL cube, Elementar Analysensysteme, Langenselbold, Germany). Organic Carbon (OC) was calculated by subtracting the C concentration of a loss on ignition sample (550 °C for 2 h) from the original C concentration. pH was measured in an equilibrated 0.01 M $CaCl_2$ solution (1:5 soil:liquid ratio). Mineral composition was measured by X-ray diffraction (XRD, $CubiX^3$, Malvern Panalytical, Malvern, United Kingdom). Trace and major metals (e.g. Fe, Mn, Cu) and Hg were extracted from soils using a 15.8 M nitric acid microwave digestion and measured using an Inductively Coupled Plasma - Mass Spectrometer (ICP–MS, 7700x, Agilent Technologies, Santa Clara, United States of America). Methylmercury was selectively extracted with HCl and dichloromethane (DCM) using an adapted method described elsewhere (Gygax et al., 2019). We modified this method to achieve high throughput (64 Samples per run) and measurements by High Pressure Liquid Chromatography (HPLC, 1200 Series, Agilent Technologies, Santa Clara, United States of America) coupled to the ICP–MS. Details on laboratory materials, extractions, analytical methods and instrumentation are provided in the supplement (Sects. S2, S3). We calculated the relative de-

https://doi.org/10.5194/bg-2020-466
Preprint. Discussion started: 1 February 2021

/methylation during the incubation as the relative difference of MeHg/Hg ratios between two time points (t) using Eq. (1).

$$De/methylation\ (\%) = \frac{\left(\frac{MeHg}{Hg}_{t_{i-1}} - \frac{MeHg}{Hg}_{t_i}\right)}{\frac{MeHg}{Hg}_{t_{i-1}}} \times 100 \quad (1)$$

2.4 Soil description.

Both soils were identified as *Fluvisols gleyic.* They have a silt loam texture, the same mineral composition but differing Hg and organic carbon (C_{org}) concentrations (Table 1). For elements relevant for Hg cycling, Hg molar ratios (Hg:Cu, Hg:C_{org}, Hg:Mn) differ between samples and soils used in similar incubation experiments (Hofacker et al., 2013; Poulin et al., 2016). We note that the $[C_{org}/Mn]_{molar}$ was 30 % higher in the LMHC soil compared to HMLC. X-Ray diffractograms of both soils are shown in Fig. S3. The soils diffractograms are overlapping each other and the qualitative analyses of the diffractograms show that the soils parental material is composed of the same five main mineral phases, Quartz, Albite, Orthoclase, Illite/Muskovite, Calcite.

2.5 Soil solution sampling and analyses

Soil solution was sampled 0.25, 1, 2, 3, 4, 5, 7, 9, 11, 14 days after the onset of each flooding period respectively (Fig. 1, Fig. S4). It was sampled though the tubing connected to the suction cup (< 10 µm pre size). The first 2 ml were sampled with a syringe and discarded to prime the system and condition the tubing. After, 4 ml were drawn through an airtight flow-through system to measure the redox potential (Hg/HgCl ORP electrode) and pH. Then, approximately 35 ml of soil solution were sampled using a self-made syringe pump system allowing for a regular flow and minimal remobilization of fine particles. We left one part of the soil solution as such (filtered by suction cup to < 10 µm) while a second part was filtered to < 0.02 µm pore size (Whatman® Anodisc 0.02 µm, Sigma-Aldrich, St. Louis, United States of America). A third part was filtered to < 0.45 µm on days 2, 5 and 9 after the onset of each flooding period. Subsequently, the samples were subdivided and treated for different analyses. They were preserved in 1 % HNO_3 for multi elemental analysis (Al, P, Cr, Mn, Fe, Ni, Cu, Zn, As, Sr, U) and in 1 % HNO_3 0.5 % HCl for Hg analysis and analyzed by ICP–MS. For major anion (Cl^-, NO_3^-, SO_4^{2-}) and cation (K^+, Na^+, Mg^{2+}, Ca^{2+}) measurements, samples were diluted 1:4 in ultra-pure water and analyzed by Ion Chromatography (Dionex Aquion™, Thermo Fisher Scientific Inc., Waltham, United States of America). Samples for Dissolved Organic Carbon (DOC), Particulate Organic Carbon POC and Total Nitrogen Bound (TN_b) were diluted 1:5 and stabilized using 10 µl of 10 % HCl and measured using an Elemental Analyzer (vario TOC cube, Elementar Analysensysteme, Langenselbold, Germany). Incubation experiment blanks were below 0.396 mM and 1.6 µM for DOC and TN_b, respectively. These relatively high blank values might originate from either the syringes or the suction cups (Siemens and Kaupenjohann, 2003). HCO_3^- concentrations were estimated based on the ionic charge balance of the soil solution using VisMinteq (https://vminteq.lwr.kth.se/). A detailed schedule and list of analyses is provided in Figure 1 and Table S2. Concentrations of specific filter fractions are labelled with suffix (e.g. $Hg_{<0.02µm}$). Particulate concentrations (0.02 µm < X < 10 µm) (PHg) and its proportion to the total (PHg_{rel}) were determined as the difference between unfiltered and filtered concentration (Table 1).

https://doi.org/10.5194/bg-2020-466
Preprint. Discussion started: 1 February 2021

209 **2.6 Characterization of Colloids (AF4)**

210 An aliquot of the soil solution was used for characterization of colloids in one out of three replicate MCs (Rep1) of
211 each treatment on days 2, 5, 9 days after the onset of each flooding period respectively. Right after sampling, the
212 aliquots were transferred to a N_2 atmosphere in a glove box. There, the samples were filtered to < 0.45 µm and pre-
213 served in airtight borosilicate headspace vials at 4 °C. Colloidal size fractions and elemental concentrations of the
214 filtrates were analyzed by Asymmetrical Flow Field-Flow Fractionation (AF4, AF2000, Postnova analytic, Lands-
215 berg am Lech, Germany) coupled to a UV_{254nm} absorbance detector (UVD), a Fluorescence detector (FLD, RF-20A,
216 Shimazu, Reinach, Switzerland) and an ICP–MS (7700x, Agilent Technologies, Santa Clara, United States of Amer-
217 ica) within 14 days after sampling. Colloids contained in 1 mL of samples were separated in a channel made of a
218 trapezoidal spacer of 350 µm thickness and a regenerated cellulose membrane with a nominal cut-off of 1 kDa used
219 as accumulation wall. The mobile phase used for AF4 elution was 10 mM NH_4NO_3 at pH 7 and was degassed prior
220 entering the channel by argon flowing. A linear decrease of crossflow from 2 to 0 mL min^{-1} over 20 min was used
221 after injecting the samples at an initial crossflow of 2.7 mL min^{-1}. At the end of a run, the crossflow was kept at 0
222 mL min^{-1} for 5 min in order to elute non-fractionated particles. Retention times were transformed into hydrodynamic
223 diameters (d_h) by an external calibration using Hemocyanin Type VIII from Limulus polyphemus hemolymph
224 (monomer d_h = 7 nm, Sigma-Aldrich) and ultra-uniform gold nanoparticles (Nanocomposix) of known d_h (19 nm
225 and 39 nm). Additionally, the elution of the smallest retention times (d_h < 10 nm) were converted into molecular
226 masses (Mw) using PSS standards (Postnova analytic, Landsberg am Lech, Germany) with Mw ranging from 1.1 to
227 64 kDa (Fig. S5), using AF4-UVD_{254nm}.
228 Fractograms obtained in Counts Per Seconds (CPS) from Time Resolved Analysis (TRA) acquisition were convert-
229 ed to µg L^{-1} using external calibrations made from a multi-element standard solution (ICP multi-element standard
230 solution VI, Merk, Darmstadt, Germany) diluted in 1 % HNO_3 or a Hg standard (ICP inorganic Hg standard solu-
231 tion, TraceCERT®, Sigma-Aldrich, St. Louis, United States of America) diluted in 0.5 % HCl 1 % HNO_3. The dif-
232 ferent size fractions were obtained by multiple extreme-shaped peak fitting, using OriginPro 2018 software
233 (OriginLab Corporation). The peaks obtained were then integrated individually, after conversion of elution time to
234 elution volume, to provide the quantity of Hg in each size fractions (Dublet et al., 2019). The analytes passing the 1
235 kDa membrane are considered as the (< 1 kDa) truly dissolved fraction. It was calculated by subtracting the concen-
236 trations of colloidal Hg recovered by AF4–ICP–MS (total integration of the Hg signals) to the total dissolved Hg
237 concentrations measured separately by ICP–MS in corresponding acidified samples. The concentration of truly dis-
238 solved Hg is displayed as $Hg_{<1kDa}$ for the rest of the article (Table 1). AF4–ICP–MS, UV_{254nm} and fluorescence sig-
239 nals were used to further characterize Hg bearing colloids, after hydrodynamic size separation by AF4. The UV_{254nm}
240 light absorption is widely used to detect organic compounds but it should be noted that part of the UV_{254nm} light
241 signal can as well originate from Fe(II) or Fe hydroxides (Dublet et al., 2019). This was not the case in this study
242 since UV_{254nm} signals were associated with C signals recorded by ICP–MS and matched the fractograms obtained by
243 the FLD detector tuned at the wavelengths specific for humic-like fluorophores. It is therefore assumed that UV_{254nm}
244 signal represents organic compounds throughout the manuscript.

https://doi.org/10.5194/bg-2020-466
Preprint. Discussion started: 1 February 2021

3. Results

3.1 Mercury dynamics (mobilization and sequestration).

In the HMLC control MCs, the pH of the soil solutions remained in a neutral to alkaline range of 8 to 8.4 throughout the whole experiment (Fig. S6). The DOC concentrations ranged between 37.5 and 106 mg L^{-1} (Fig. 2h). A continuous soil reduction was observed with completed NO_3^- reduction and the onset of Mn release at day 7 of the main incubation (Figs. 2d and S7). An increase of both $Hg_{<0.02\mu m}$ and $Hg_{<10\mu m}$ concentrations was simultaneous to the Mn release (Figs. 2a-e). Mean $Hg_{<0.02\mu m}$ concentration peaked on day 9 (17.1 ± 2.3 µg L^{-1} $Hg_{<0.02\mu m}$) and slightly decreased towards the end of the first flooding period on day 14 (13.7 ± 4.9 µg L^{-1} $Hg_{<0.02\mu m}$). The proportion of particulate Hg, $PHg_{rel.}$, gradually decreased from a maximum of 88 % to a minimum of 25 % at the end of the first flooding (Fig. 2c). $Cu_{<0.02\mu m}$ concentrations increased up to 88.2 ± 17.5µg L^{-1} within the first 4 days and then gradually decreased to 30.6 ± 3.54 µg L^{-1} at day 14 (Fig. 2e).

During the second flooding period, individual MCs behaved differently in the HMLC control treatment. The differences of soil solution E_h and redox sensitive trace metals (e.g. Cu, Mn, Hg, Fe, Cr) were apparent from the start of the second flooding (Figs. 2f-g, S8). Contrastingly, DOC concentrations and pH remained similar between incubators (Fig. 2h). Two replicates (Rep1; Rep3) showed a pronounced increase of E_h after the draining period (Fig. 2i). The Rep1 showed a depletion of Mn in soil solution indicating the formation of Mn oxide minerals but values obtained for $Hg_{<0.02\mu m}$and $Mn_{<0.02\mu m}$ were then increased and peaked at 23.6 µg L^{-1} and 448 µg L^{-1} respectively during the second flooding. The $PHg_{rel.}$ decreased from 60 % to 30 %, and $Cu_{<0.02\mu m}$ concentrations were high (88.4 µg L^{-1}) at the onset but decreased to lower levels (11.8 µg L^{-1}). Further, the E_h of this MC remained high (150 to 300 mV) in this period. The E_h of Rep2 was lower (between 28 and 120 mV), Mn remained at the same level before and after draining phase, and no second release of Hg was observed. The Rep2 showed a release of Fe indicating the onset reduction of Fe oxyhydroxides, analogous to the Mn release in Rep1. The $PHg_{rel.}$ remained between 60 and 75 % in this MC. In Rep3, Mn remained at the same level before and after the draining period. During the second flooding, this MC showed a slightly lower release of Hg compared to Rep1, peaking at 10.9 µg L^{-1}, and associated to a decrease of $PHg_{rel.}$ from 60 % to 30 % and showed a faster decrease in DOC compared to the two other MCs (Fig. 2h).

In the cornfield soil MC with manure addition (HMLC +MNR) pH remained in the range of 8 to 8.35 with minor fluctuations throughout the experiment. DOC concentrations were ranging between 72.2 and 134 mg L^{-1} (Fig. 2h). This was significantly higher (3 to 43 mg L^{-1}) than in HMLC control. Soil solution redox potential decreased rapidly from approx. E_h 300 mV to 5.27 ± 14.4 mV within the first 14 days of the incubation in the HMLC +MNR treatment. It remained constant at 14.3 ± 8.12 mV during the second flooding period. Release of Mn and Hg started at day 2 of the main incubation once NO_3^- reduction was completed (Figs. 2, S6). Concentration of $Hg_{<0.02\mu m}$ peaked on day 4 at 15.9 ± 1.4 µg L^{-1}. By day 14, the Hg concentrations were close to the initial levels (1.73 ± 0.83 µg L^{-1} $Hg_{<0.02\mu m}$) and remained low the rest of the incubation experiment. The PHg_{rel} decreased to approx. 40 % during the release of Hg but was > 60 % before and after. With the onset of the decrease in soil solution Hg concentration, we visually observed black precipitates in the incubators with added manure. Unlike the HMLC control, MCs triplicates of HMLC +MNR behaved similarly during both flooding periods. No Hg release was observed during the second flooding.

https://doi.org/10.5194/bg-2020-466
Preprint. Discussion started: 1 February 2021


Biogeosciences Discussions Open Access EGU

LMHC differed from HMLC in soil solution Hg dynamics. In both treatments (LMHC and LMHC +MNR), pH remained neutral but gradually decreased from 8.2 to 7.5 during the incubation (Fig. S6). Soil reduction progressed rapidly from a max of 332 mV at day 3 to -14.3 mV at day 14 (Fig. 3f). During the second flooding E_h stayed in the range of - 2.3 to 34.5 mV. Mn as well as DOC concentrations gradually increased during the first flooding period (Fig. 3d-e). Soil solution $Hg_{<0.02\mu m}$ concentration (25 – 160 ng L^{-1}) are two orders of magnitude lower than in the HMLC runs (Fig. 3a). Both $Hg_{<0.02\mu m}$ and $Hg_{<10\mu m}$ decreased gradually during the first flooding period (Figs. 3a-b). No other soil solution parameter followed the trend of Hg. In both treatments but the $PHg_{rel.}$ differed clearly between first flooding (> 65 %) and second flooding period (<< 50 %) (Fig. 3c).

3.2 Colloidal Hg (AF4)

Hg bearing colloids were detected in all soil solution samples of HMLC incubations. Due to low signal to noise ratios (< 3) we did not detect colloidal Hg in samples of the LMHC incubations. The proportion of truly dissolved $Hg_{<1kDa}$ varied between 0 % and 67 % in the HMLC control experiment and was high during the times of Hg release to soil solution (Fig. 4). In the HMLC +MNR treatment, $Hg_{<1kDa}$ were lower and ranged between 0 % and 29 %. The colloidal Hg can be divided into 3 main fractions (Fig. 5). The first Hg colloidal fraction showed a main peak ranging between 1 – 40 kDa (d_h < 6 nm) and was associated with UV_{254nm}-absorbing compounds and various metals (Mn, Fe, Cu, Ni, Zn). This fraction was interpreted as humic substance type Hg–NOM. The proportion of this colloidal Hg fraction varied with no specific trends from 11.5 to 23.3 % in HMLC and 13.6 to 38.6 % in HMLC +MNR thoughout the course of the experiment. A second fraction of Hg colloids ranged between 6 nm and 20 nm. This well-defined size fraction was eluting in the tail of the first fraction for other metals (e.g. Fe, Mn, Cu) but did not overlap with UV_{254nm} and fluorescence signals (Fig. 5). This fraction could not be chemically defined but is hypothesized to consist of $HgS_{(s)}$ colloids. In the HMLC control treatment, we observed a decrease in the proportion of these inorganic colloids from 28 % at the onset to 15.3 % at the end of the incubation (Fig. 4). In the HMLC +MNR treatment, the proportion of this fraction ranged between 29.5 % and 41.9 % during the first flooding and could not be detected during the second flooding. Further, we observed a third colloidal fraction that continued to elute after the stop of the AF4 crossflow and it included colloids in the range of 30 – 450 nm (effective cut-off of the filter used for the sample preparation). In some cases, this fraction was better fitted using two overlapping populations (Fig. 5, Figs. S9-S12). In all the cases, Hg signal was associated with those of other metals and a slight bump of the UV_{254nm} signal but more specifically an increase of fluorescence signal associated to protein-like fluorophores. This fraction decreased continuously in the HMLC control treatment during the incubation from 32.4 % at day 2, to 5.6 % at day 9 and stood under 9.1 % during the rest of the incubation. By contrast, the HMLC +MNR showed an increase in the proportion of this fraction from 7.3% at day 2 to 25.3 % by the end of the incubation (Fig. 4). The deconvolution of the fractograms included an intermediate fraction of Hg bearing colloids ranging between d_h = 6 nm and d_h = 450 nm depending on the sample. This fraction was added to refine the fractogram fittings but could not directly be associated to another measured metal. This indicates that this population overlap a more polydispersed Hg particle population although in some cases the presence of small Hg particles dominates. This broad fraction was not detected in HMLC +MRN treatments during the first flooding but made up > 30 % during the second flooding.

https://doi.org/10.5194/bg-2020-466
Preprint. Discussion started: 1 February 2021

3.3 Net Hg methylation/demethylation

Soil MeHg levels fluctuated over the course of the incubation experiment, Fig. 6 and Table 2. Highest net-methylation was observed during the first flooding period for the treatments with MNR (up to + 81%) and during the draining phase for the treatments without MNR (up to + 73.1 %). We observed a significant decrease of MeHg/Hg and absolute MeHg concentrations in all incubators during the second flooding period (Fig. 6). In all MCs, MeHg/Hg increased by a factor of 1.18 to 1.36 throughout the incubation.

4. Discussion

4.1 Mercury release and sequestration.

Cornfield soil (HMLC) and pasture field soil (LMHC) behaved very differently in this incubation experiment and will be discussed separately. In the cornfield soil Hg and Mn releases were simultaneous and started when soil solution E_h entered the field of Mn reduction below approx. 300mV (Figs. 2a, 2h), strongly suggesting that this Hg pool was adsorbed to Mn-oxyhydroxides. The simultaneous decrease of the $PHg_{rel.}$ and $PMn_{rel.}$ indicates that Hg was adsorbed on both Mn-oxyhydroxides from soil and suspended particles (Figs. 2c and 2e). No other soil solution parameter (e.g. DOC) was directly related to the release of Hg. In the fluvisol of our study area, Hg mobilization is thus not driven by the mobilization of DOM unlike in peat soils, Histosols or Podsols in boreal environments (Åkerblom et al., 2008; Kronberg et al., 2016; Jiskra et al., 2017). Likewise we did not observe a mobilization of Hg together with Cu as reported earlier (Hofacker et al., 2013). This is explained by the comparably high Hg/Cu_{molar} ratio in our soil matrix. After Hg release, Hg concentrations remained high and the particulate Hg fraction low throughout the experiment. This illustrates that the released pool of Hg mainly originated from Mn-oxyhydroxides and less from suspended POM nor particulate sulfide minerals in the cornfield soil. However, the pool bound to Mn-oxyhydroxides is relatively small. In neighboring soils the main Hg pool was previously reported as $HgS_{(s)}$ and Hg complexed by recalcitrant NOM (Grigg et al., 2018). Earlier studies assumed that 0.1 to 0.6 % (w/w) of NOM was reduced sulphur with high affinity to Hg (Grigg et al., 2018; Ravichandran, 2004). Following this assumption, reduced sulfur groups of the cornfield soil NOM could sorb between 11.9 to 71.9 mg kg^{-1} of Hg. The soils high Hg concentration (44.8 mg L^{-1}) suggest, that soil NOM thiol sites are likely saturated in terms of Hg. Therefore, saturated NOM sorption sites are not competing with Mn-oxyhydroxide sorption sites, resulting in a substantial Mn-oxyhydroxide bound Hg-pool. This leads to a higher mobility of Hg upon reductive dissolution of Mn-oxyhydroxide compared to fluvisols used in other incubation studies (Hofacker et al., 2013; Poulin et al., 2016).

During the second flooding phase, HMLC control runs showed a higher variability in redox sensitive soil solution parameters (Fig. 2). This might be explained as a.) a shift in microbial communities, b.) disturbance of the soil column by invasive soil sampling in between the flooding periods or c.) uneven draining of the pore space after the first flooding. It can also reflect how redox cycle can be easily affected *in situ*. We suggest that the second release of Mn and Hg in Rep1 is due to Mn re-oxidation during the draining period and a second reductive dissolution of Mn oxyhydroxides upon reflooding. This is supported by the elevated E_h at the onset of the second flooding. The HMLC control Rep3 showed a second release of Hg without a remobilization of Mn. Changing redox conditions have been

https://doi.org/10.5194/bg-2020-466
Preprint. Discussion started: 1 February 2021


Biogeosciences Discussions Open Access EGU

353 shown to enhance microbial respiration and therefore NOM degradation (Sunda and Kieber, 1994). Further, Mn
354 oxidation was shown to enhance the degradation of larger NOM to LMW–NOM (Jones et al., 2018). Thus, we in-
355 terpret the second Hg release in Rep 3 as a degradation/mineralization of NOM that bound Hg.
356 The addition of manure accelerated the release of Hg through reductive dissolution of Mn oxyhydroxides. Mercury
357 was released 4 day earlier in the +MNR group compared to the control. We interpret this as an effect of additional
358 organic carbon of the liquid manure acting as electron donor enhancing microbial activity. In the manure treatment,
359 we observed a fast decrease of Hg concentration and a constantly high proportion of particulate $Hg_{0.02\mu m\text{-}10\mu m}$ even
360 after the plateau of Mn concentration in soil solution and the decrease of particulate Mn. The addition of manure
361 represents an addition of 0.3 g of fresh NOM to the MCs. It is a source of POM (manure was sieved to < 500 µm)
362 and increased DOC approximately by 20 mg L^{-1}. Therefore, we explain the decrease of Hg by a continuous com-
363 plexation of mobilized Hg with the added NOM of the manure. The freshly added manure served as a source of new
364 thiol sites. Adsorption of Hg is directed towards larger more thiol rich NOM (Liang et al., 2019) and different ligand
365 exchange reactions (e.g. carboxyl-groups to thiol groups) happen within days (Miller et al., 2009; Chiasson-Gould et
366 al., 2014). In addition, we visually observed black precipitated at the first day of Hg decrease in the MCs with ma-
367 nure addition (Fig. S13) indicating the precipitation of sulfide mineral particles. Although, E_h measurements did not
368 indicate sulphate reduction, the formation of sulfide minerals in micro- and meso-pores are possible. Furthermore,
369 the formation of $HgS_{(s)}$ from Hg–NOM was reported even under oxic-conditions (Manceau et al., 2015). In both
370 scenarios the addition of manure would accelerate the process either by promoting soil reduction or as additional
371 source of NOM.
372 Hofacker et al., 2013 reported a quantitatively relevant incorporation of Hg into metallic Cu^0 particles. However, we
373 do not consider this a relevant pathway, due to the relatively high Hg/Cu_{molar} ratio in our soil compared to Hofacker
374 et al., 2013. Although the simultaneous decrease of Hg and Cu may be interpreted as the immobilization of Hg
375 though incorporation into metallic Cu particles, i) we did not observe the formation of colloidal Cu associated with
376 Hg (Sect. 6.2) and ii) relatively high Hg/Cu molar ratios indicate that the decrease of Hg in the soil solution cannot
377 be solely explained by this mechanism as Hg would be marginally incorporated metallic Cu^0 particles.
378 As well, Hg in soil solutions may be volatilized by reduction of Hg^{2+} to Hg^0 (Hindersmann et al., 2014). Our exper-
379 imental design did not allow for quantification of gaseous Hg^0 and it may have exited the MCs since they were only
380 sealed with parafilm. Reduction of Hg^{2+} may happen both biotically and abiotically. The former process is a detoxi-
381 cation mechanism of bacteria carrying *merA* genes in Hg polluted environments. Biotic volatilization has been ob-
382 served in neighboring soils of our sampling site (Frossard et al., 2018). Organic amendments and high Hg levels
383 have been shown to increase the abundance of Hg reducing bacteria (Hu et al., 2019). However, it is unlikely that
384 Hg reduction can solely explain the decrease of Hg in the soil solution in our microcosms. We therefore interpret the
385 decrease in Hg concentration to be due to a combination of manure NOM complexation and sequestration together
386 with the formation $HgS_{(s)}$ during flooding.
387 In the pasture field soil, soil solution Hg concentrations remained at low levels (< 0.16 µg L^{-1} $Hg_{<0.02\mu m}$) during the
388 whole experiment in both treatments (Fig. 3a). Unlike in the cornfield soil, we did not observe a simultaneous re-
389 lease of Hg upon Mn reduction (Fig. 3d). We explain this with the not completely Hg saturated NOM in this soil, if

https://doi.org/10.5194/bg-2020-466
Preprint. Discussion started: 1 February 2021

we assume that 0.1 – 0.6 % (w/w) of NOM was reduced S with high affinity to Hg (Grigg et al., 2018; Ravichandran, 2004; Skyllberg, 2008). Thus, the pasture field soil has a rather limited pool of labile Hg compared to the cornfield soil. Both $Hg_{<0.02\mu m}$ and $Hg_{<10\mu m}$ negatively correlate with the sum of sampled soil solution (R^2 = -0.841, p= <0.001) during both flooding periods. Both $Hg_{<0.02\mu m}$ and $Hg_{<10\mu m}$ pools decreased fast. This suggests that a concentration gradient between supernatant artificial rainwater and the soil solution contributed to the fast exhaustion of the small labile Hg pool in pasture field soil. The presence of this concentration gradient in our incubation setup is confirmed by the continuously decreasing concentrations of conservative ions (Cl^-, Na^+, K^+) in soil solutions of the HMLC runs (Sect. S5.2, Figs. S6, S7). The relatively high proportion of particulate Hg vastly decreased during the draining period (Fig. 3b,c) and we speculate that this change is a result of the mobilization of the POM–Hg pool by mineralization/degradation of NOM which sorbed Hg during the draining period (Jones et al., 2018). In summary, flooding of the pasture field soils did mobilize only a small pool of particulate bound Hg which was exhausted within the first flooding period.

4.2 Colloidal Hg

In the absence of manure, AF4 results show that the Hg released from Mn-oxyhydroxides (Sect. 6.1.2) was dominated by truly dissolved Hg (Hg^{2+} or LMW–NOM–Hg) (Fig. 4). The high Cl^- concentrations (up to 800 mg L^{-1}, Fig. S14) likely influenced the Hg speciation in the soil solution, as chloride is a main complexant for Hg^{2+} (Li et al., 2020; Gilli et al., 2018). During Hg release, the proportions of larger Hg colloids (> 25 nm) decreased. The stable proportion of humic substances bound Hg and inorganic Hg colloids between 6 nm and 25 nm indicates that once released no major adsorption or aggregation of truly dissolved Hg and larger colloidal Hg occurs. Additional complexation of Hg by DOM can be excluded if we assume the saturation state of thiol-sites of the NOM pool in the soil (Sect. 6.1.2). These observations illustrates the remarkably high Hg mobility and potentially increased bioavailability (proportion of truly dissolved Hg) to Hg metabolizing microorganisms compared to other studies (Hofacker et al., 2013; Poulin et al., 2016). These authors did either not observe Hg in truly dissolved form or a decreased to low levels within the first days of incubation. Overall, the released Hg from cornfield soil shows a high mobility and might represent a possible threat to downstream ecosystems and a source for Hg methylating bacteria. However, the released Hg from soil matrix represents a rather small pool of the total Hg (44.8 mg kg^{-1}). Further work would be needed to establish a Hg flux model to better understand *in situ* soil Hg mobility in these soils.

The manure addition had a key effect on the proportions of colloidal fractions in soil solution, and overall led to a low proportion of truly dissolved fraction (Fig. 4). The Hg colloidal distribution was dominated by the presence of large fractions (30 - 450 nm). Larger organic acids with high aromaticity usually contain higher proportions of thiols groups than smaller molecules and selectively complex Hg (Haitzer et al., 2002). This suggests that Hg complexation is kinetically driven and it can shifts from LMW–DOM to larger NOM and larger aggregates of POM as supported by earlier incubation experiments (Poulin et al., 2016). We therefore interpret the relative increase of Hg colloids with d_h = 30 – 450 nm (Fig. 4) as a complexation of the released dissolved $Hg_{<1kDa}$ by thiol groups of NOM in larger clay-organo-metal complexes during the experiment.

https://doi.org/10.5194/bg-2020-466
Preprint. Discussion started: 1 February 2021

425 The onset of sulfate reduction (Rivera et al., 2019) as well as the interaction of Hg with NOM (Manceau et al., 2015)
426 may cause the precipitation of Hg bearing sulfide minerals and nanoparticles ($FeS_{(s)}$, ß-$HgS_{(s)}$) (Sect. 6.1.1). We
427 therefore suggest that the distinct fraction of colloids with d_h = 6 – 25 nm is $HgS_{(s)}$. The AF4 fractograms show the
428 presence of these colloids during the first flooding period but not during the second flooding one. Moreover, the
429 proportion of the intermediate fraction increased in the second flooding. Although the presence of e.g. humic sub-
430 stances and larger NOM was shown to narrow the size range of $HgS_{(s)}$ nanoparticles precipitating from solution
431 (Aiken et al., 2011) , through time, these colloids may grow, aggregate and form clusters in a wide size distribution
432 (Deonarine and Hsu-Kim, 2009). We explain the disappearance of monodisperse colloids by their aggregation dur-
433 ing the draining period, leading also to sequestration of Hg in the soil matrix, without remobilization during the
434 second flooding.

435 **4.3 Net-methylation during flooding-draining experiment.**

436 The studied soils show uncommonly high initial MeHg levels (6.4 – 26.9 µg kg^{-1}) when compared to other highly
437 polluted mining or industrial legacy sites (Horvat et al., 2003; Neculita et al., 2005; Qiu et al., 2005; Fernández-
438 Martínez et al., 2015). Still, we observed significant MeHg production during the first 28 days of the incubation
439 resulting in even higher MeHg concentrations of up to (Table 3; Fig. 6). Soils treated with manure showed a faster
440 methylation with highest net methylation during the first flooding period. Controls showed highest net methylation
441 during the draining period and reached similar levels of MeHg at the start of the second flooding on day 28 (Fig. 6).
442 For cornfield soil (HMLC), both treatments show a high concentration of highly bioavailable Hg ($Hg_{<0.02µm}$ and
443 $Hg_{<1kDa}$) in soil solution during the first flooding. Methylation is therefore rather limited by cellular uptake of Hg or
444 the microbial activity of methylating microorganisms than bioavailability. Thus, we interpreted the higher methyla-
445 tion rate of the manure treatments as a result of higher microbial activity. However, we did neither assess the activity
446 nor the abundance of Hg methylating bacteria. In the control run, a substantial part of Hg was methylated during the
447 draining period. This indicates that even if low concentrations of Hg is released (LMHC MCs day 14: $Hg_{<0.02µm}$ < 50
448 ng L^{-1}) a substantial amount of Hg can be methylated. Micro- and meso pore spaces with steep redox gradients act as
449 ideal environments for microbial methylation even in drained and generally aerobic system (e.g. HMLC control
450 during the draining period).
451 Further, we observed a net demethylation in all MCs during the second flooding period. Oscillating net
452 de/methylation in environments characterized by flood-drought-flood cycles have been reported earlier (Marvin-
453 DiPasquale et al., 2014). Degradation of MeHg was reported to happen either abiotically by photodegradation or
454 biotically by chemotrophic reductive or oxidative demethylation by microorganisms carrying the *mer*-operon
455 (Grégoire and Poulain, 2018). A photodegradation of MeHg can be excluded as the experiment was conducted in the
456 dark. However, demethylation could have happened as biotic reductive demethylation. A possible explanation is a
457 MeHg detoxification reaction by microorganisms carrying the *mer*-operon (*merB*) (Hu et al., 2019; Frossard et al.,
458 2018; Dash and Das, 2012). However, we can only hypothesize about demethylation mechanisms, as neither com-
459 munities (DNA) nor gene expression (mRNA)s dynamic in the soils were analyzed during the experiment.

https://doi.org/10.5194/bg-2020-466
Preprint. Discussion started: 1 February 2021

4.4 Experimental Limitations

Incubation experiments on a laboratory scale are a common way to study the changes in mobility of trace elements in floodplain soils (Gilli et al., 2018; Frohne et al., 2011; Poulin et al., 2016; Abgottspon et al., 2015). These study designs allow for controlled conditions and replicable results. However, controlled experiments usually fail to cover the complexity of a real floodplain soil system (Ponting et al., 2020). Our study design did not involve temperature gradients, realistic hydrological flow conditions or intact soil structure. In this study, the artificial rainwater and the soil were equilibrated by shaking for a few minutes. However, the equilibration appeared to be incomplete with respect to highly soluble chloride bearing minerals for the experiment with cornfield soil (Fig. S14). This is supported by the temporal patterns of conservative ions (Cl^-, K^+ and Na^+) in soil solution (Figs. S6, S7) and the difference in Cl^- concentration between the soil solutions at t = 6 h and the same water-soil mixture shaken for 6 h (Fig. S14). These patterns were only visible due to high levels of these elements to start with, which most likely stem form a fertilisation event that must have taken place just prior to sampling the soil. Nonetheless, they show that soil solution sampling removed a considerable amount of dissolved elements and the decrease in soil solution concentration of some elements can be linked to the sampling, making their interpretation difficult. The infiltration of surface water further led to a dilution of the soil solution. However, the release of soil bound elements (e.g. As, Hg, Mn, Fe) by e.g. reductive dissolution, do not seem to be directly affected by this mechanism. It should also be noted that high initial Cl^- concentrations in the soil solution, may influence Hg solubility since Cl^- is a complexant for Hg^{2+} (Li et al., 2020) and this warrants further studies on the role of inorganic fertilisation on Hg mobility.

5. Conclusions

We studied the effect of manure addition on the mobility of Hg in soil during a flooding-draining experiment. Further, we observed the formation and size distribution changes of Hg colloids in soil solution by AF4–ICP–MS. The results of this study show that manure addition has a distinct effect on 1.) temporal Hg release and sequestration, 2.) Hg complexation with fresh NOM and colloid formation and 3.) net methylation dynamics in polluted and periodically flooded soils.

In the cornfield soil (HMLC), Hg was mobilized upon reductive dissolution of Mn hydroxides. The application of manure accelerated the release of Hg, facilitated the formation of colloidal Hg and exhausted the mobile Hg pool within the first 7 days of flooding. This prevented Hg remobilization during the second flooding period. In pasture field (LMHC) soil Hg was mainly released as particulate bound Hg presumably due to the higher soil organic carbon content. This relatively small pool of particulate Hg was exhausted within the first flooding period. In both soils, MeHg formation upon flooding-draining cycles suggest that the changes of redox conditions enhance methylation of a substantial part of the Hg pool. However, MeHg declines from the soil by either advective transport of dissolved MeHg in the soil column or by reductive demethylation. Due to the wide differences in bioavailable Hg between treatments and soils we suggest that the temporal changes net-methylation are limited by microbial activity of Hg methylators. Their activity appears to be facilitated by fresh manure addition.

https://doi.org/10.5194/bg-2020-466
Preprint. Discussion started: 1 February 2021

494 The release of Hg from polluted soils to downstream ecosystems does depend on both biogeochemical conditions as
495 well as on hydrological transport. Our experiment shows that redox oscillations (flooding-draining-flooding cycles)
496 of a polluted floodplain soil are likely to induce pulses of both Hg and MeHg to the downstream ecosystems. This is
497 supported with earlier studies (Poulin et al., 2016; Frohne et al., 2012; Hofacker et al., 2013). In NOM poor agricul-
498 tural soils, the application of additional NOM in form of manure may reduce the mobilization and contribute to the
499 transformation of Hg towards less mobile species, especially during low flow conditions. Overall, more work is
500 needed to understand the mobilization of Hg in polluted areas. More precisely, field trials integrating biogeochemi-
501 cal processes, hydrological transport and Hg soil-air exchange are needed in order to establish Hg flux models to
502 better understand *in situ* soil Hg mobility.
503

504 **Data availability.**

505 Details of analytical methods, AF4–ICP–MS fractograms are given in the Supplement. A complete dataset of the
506 data used in this study is accessible at http://doi.org/10.5281/zenodo.4058676
507

508 **Acknowledgements.**

509 We acknowledge P. Neuhaus, J. Caplette, K. Trindade, K. Kavanagh, and D. Fischer for the help in the laboratory.
510 T. Erhardt at the Climate and Environmental Physics (CEP) at University of Bern for the ICP–TOF–MS analyses.
511 Stefan Westermann at the Dienststelle für Umweltschutz (DUS) of the Canton Wallis for the help with site selection
512 and sampling permissions. Soil temperatures have been provided by MeteoSwiss, the Swiss Federal Office of Mete-
513 orology and Climatology. Klaus Jarosch and Moritz Bigalke of the soil science group at the Institute of Geography
514 at University of Bern for the advises during the writing process.

515 **Author contribution.**

516 AM and LG designed the study. LG and AW preformed the incubation experiments. LG and IW performed labora-
517 tory analyses. LG and IW performed the data analysis. AM and VS supervised and financed the study. LG prepared
518 the manuscript with contributions from all co-authors.

519 **Financial support.**

520 This work was funded the Swiss National Science Foundation (SNSF, Nr. 163661). VS and IW acknowledge the
521 financial support of the SNSF R'Equip project Nr. 183292.

https://doi.org/10.5194/bg-2020-466
Preprint. Discussion started: 1 February 2021

522

523 **References**

524 Abgottspon, F., Bigalke, M., and Wilcke, W.: Fast colloidal and dissolved release of trace elements in a carbonatic
525 soil after experimental flooding, Geoderma, 259-260, 156–163, doi:10.1016/j.geoderma.2015.06.005, 2015.
526 Aiken, G. R., Hsu-Kim, H., and Ryan, J. N.: Influence of dissolved organic matter on the environmental fate of
527 metals, nanoparticles, and colloids, Environmental science & technology, 45, 3196–3201,
528 doi:10.1021/es103992s, 2011.
529 Åkerblom, S., Meili, M., Bringmark, L., Johansson, K., Kleja, D. B., and Bergkvist, B.: Partitioning of Hg Between
530 Solid and Dissolved Organic Matter in the Humus Layer of Boreal Forests, Water Air Soil Pollut, 189, 239–252,
531 doi:10.1007/s11270-007-9571-1, 2008.
532 AMAP/UN Environment: Technical Background Report for the Global Mercury Assessment 2018, Arctic Monitor-
533 ing and Assessment Programme, Oslo, Norway/UN Environment Programme, Chemicals and Health Branch,
534 Geneva, Switzerland, Geneva, Switzerland, 426 pp., 2019.
535 Amos, H. M., Jacob, D. J., Streets, D. G., and Sunderland, E. M.: Legacy impacts of all-time anthropogenic emis-
536 sions on the global mercury cycle, Global Biogeochem. Cycles, 27, 410–421, doi:10.1002/gbc.20040, 2013.
537 Beckers, F. and Rinklebe, J.: Cycling of mercury in the environment: Sources, fate, and human health implications:
538 A review, Critical Reviews in Environmental Science and Technology, 23, 1–102,
539 doi:10.1080/10643389.2017.1326277, 2017.
540 Biester, H., Müller, G., and Schöler, H.: Binding and mobility of mercury in soils contaminated by emissions from
541 chlor-alkali plants, Science of The Total Environment, 284, 191–203, doi:10.1016/S0048-9697(01)00885-3,
542 2002.
543 Bigham, G. N., Murray, K. J., Masue-Slowey, Y., and Henry, E. A.: Biogeochemical controls on methylmercury in
544 soils and sediments: Implications for site management, Integrated environmental assessment and management,
545 13, 249–263, doi:10.1002/ieam.1822, 2017.
546 Bravo, A. G., Bouchet, S., Tolu, J., Björn, E., Mateos-Rivera, A., and Bertilsson, S.: Molecular composition of or-
547 ganic matter controls methylmercury formation in boreal lakes, Nature communications, 8, 14255,
548 doi:10.1038/ncomms14255, 2017.
549 Chiasson-Gould, S. A., Blais, J. M., and Poulain, A. J.: Dissolved organic matter kinetically controls mercury bioa-
550 vailability to bacteria, Environmental science & technology, 48, 3153–3161, doi:10.1021/es4038484, 2014.
551 Deonarine, A. and Hsu-Kim, H.: Precipitation of Mercuric Sulfide Nanoparticles in NOM-Containing Water: Impli-
552 cations for the Natural Environment, Environ. Sci. Technol., 43, 2368–2373, doi:10.1021/es803130h, 2009.
553 Driscoll, C. T., Mason, R. P., Chan, H. M., Jacob, D. J., and Pirrone, N.: Mercury as a global pollutant: Sources,
554 pathways, and effects, Environmental science & technology, 47, 4967–4983, doi:10.1021/es305071v, 2013.
555 Drott, A., Lambertsson, L., Björn, E., and Skyllberg, U.: Importance of Dissolved Neutral Mercury Sulfides for
556 Methyl Mercury Production in Contaminated Sediments, Environ. Sci. Technol., 41, 2270–2276,
557 doi:10.1021/es061724z, 2007.

https://doi.org/10.5194/bg-2020-466
Preprint. Discussion started: 1 February 2021

558 Dublet, G., Worms, I., Frutschi, M., Brown, A., Zünd, G. C., Bartova, B., Slaveykova, V. I., and Bernier-Latmani,
559 R.: Colloidal Size and Redox State of Uranium Species in the Porewater of a Pristine Mountain Wetland, Envi-
560 ronmental science & technology, 53, 9361–9369, doi:10.1021/acs.est.9b01417, 2019.
561 Eklöf, K., Bishop, K., Bertilsson, S., Björn, E., Buck, M., Skyllberg, U., Osman, O. A., Kronberg, R.-M., and Bravo,
562 A. G.: Formation of mercury methylation hotspots as a consequence of forestry operations, The Science of the
563 total environment, 613-614, 1069–1078, doi:10.1016/j.scitotenv.2017.09.151, 2018.
564 Fernández-Martínez, R., Larios, R., Gómez-Pinilla, I., Gómez-Mancebo, B., López-Andrés, S., Loredo, J., Ordóñez,
565 A., and Rucandio, I.: Mercury accumulation and speciation in plants and soils from abandoned cinnabar mines,
566 Geoderma, 253-254, 30–38, doi:10.1016/j.geoderma.2015.04.005, 2015.
567 Frohne, T., Rinklebe, J., Diaz-Bone, R. A., and Du Laing, G.: Controlled variation of redox conditions in a flood-
568 plain soil: Impact on metal mobilization and biomethylation of arsenic and antimony, Geoderma, 160, 414–424,
569 doi:10.1016/j.geoderma.2010.10.012, 2011.
570 Frohne, T., Rinklebe, J., Langer, U., Du Laing, G., Mothes, S., and Wennrich, R.: Biogeochemical factors affecting
571 mercury methylation rate in two contaminated floodplain soils, Biogeosciences, 9, 493–507, doi:10.5194/bg-9-
572 493-2012, 2012.
573 Frossard, A., Donhauser, J., Mestrot, A., Gygax, S., Bååth, E., and Frey, B.: Long- and short-term effects of mercury
574 pollution on the soil microbiome, Soil Biology and Biochemistry, 120, 191–199,
575 doi:10.1016/j.soilbio.2018.01.028, 2018.
576 Gilli, R., Karlen, C., Weber, M., Rüegg, J., Barmettler, K., Biester, H., Boivin, P., and Kretzschmar, R.: Speciation
577 and Mobility of Mercury in Soils Contaminated by Legacy Emissions from a Chemical Factory in the Rhône
578 Valley in Canton of Valais, Switzerland, Soil Syst., 2, 44, doi:10.3390/soilsystems2030044, 2018.
579 Gilmour, C. C., Podar, M., Bullock, A. L., Graham, A. M., Brown, S. D., Somenahally, A. C., Johs, A., Hurt, R. A.,
580 Bailey, K. L., and Elias, D. A.: Mercury methylation by novel microorganisms from new environments, Envi-
581 ronmental science & technology, 47, 11810–11820, doi:10.1021/es403075t, 2013.
582 Glenz, C. and Escher, J.-R.: Voruntersuchung von belasteten Standorten: Histoische Untersuchung Objekt Gross-
583 grundkanal, FUAG-Forum Umwelt AG, Visp, Switzerland, 89 pp., 2011.
584 Graham, A. M., Aiken, G. R., and Gilmour, C. C.: Dissolved organic matter enhances microbial mercury methyla-
585 tion under sulfidic conditions, Environmental science & technology, 46, 2715–2723, doi:10.1021/es203658f,
586 2012.
587 Graham, A. M., Aiken, G. R., and Gilmour, C. C.: Effect of dissolved organic matter source and character on micro-
588 bial Hg methylation in Hg-S-DOM solutions, Environmental science & technology, 47, 5746–5754,
589 doi:10.1021/es400414a, 2013.
590 Grégoire, D. S. and Poulain, A. J.: Shining light on recent advances in microbial mercury cycling, FACETS, 3, 858–
591 879, doi:10.1139/facets-2018-0015, 2018.
592 Grigg, A. R. C., Kretzschmar, R., Gilli, R. S., and Wiederhold, J. G.: Mercury isotope signatures of digests and
593 sequential extracts from industrially contaminated soils and sediments, The Science of the total environment,
594 636, 1344–1354, doi:10.1016/j.scitotenv.2018.04.261, 2018.

https://doi.org/10.5194/bg-2020-466
Preprint. Discussion started: 1 February 2021

595 Guedron, S., Grangeon, S., Lanson, B., and Grimaldi, M.: Mercury speciation in a tropical soil association; Conse-
596 quence of gold mining on Hg distribution in French Guiana, Geoderma, 153, 331–346,
597 doi:10.1016/j.geoderma.2009.08.017, 2009.
598 Gygax, S., Gfeller, L., Wilcke, W., and Mestrot, A.: Emerging investigator series: mercury mobility and methylmer-
599 cury formation in a contaminated agricultural flood plain: influence of flooding and manure addition, Environ-
600 mental science. Processes & impacts, 21, 2008–2019, doi:10.1039/c9em00257j, 2019.
601 Haitzer, M., Aiken, G. R., and Ryan, J. N.: Binding of mercury(II) to dissolved organic matter: the role of the mer-
602 cury-to-DOM concentration ratio, Environmental science & technology, 36, 3564–3570,
603 doi:10.1021/es025699i, 2002.
604 Hindersmann, I., Hippler, J., Hirner, A. V., and Mansfeldt, T.: Mercury volatilization from a floodplain soil during a
605 simulated flooding event, J Soils Sediments, 14, 1549–1558, doi:10.1007/s11368-014-0908-2, 2014.
606 Hofacker, A. F., Behrens, S., Voegelin, A., Kaegi, R., Lösekann-Behrens, T., Kappler, A., and Kretzschmar, R.:
607 Clostridium Species as Metallic Copper-Forming Bacteria in Soil under Reducing Conditions, Geomicrobiology
608 Journal, 32, 130–139, doi:10.1080/01490451.2014.933287, 2015.
609 Hofacker, A. F., Voegelin, A., Kaegi, R., and Kretzschmar, R.: Mercury mobilization in a flooded soil by incorpora-
610 tion into metallic copper and metal sulfide nanoparticles, Environmental science & technology, 47, 7739–7746,
611 doi:10.1021/es4010976, 2013.
612 Hojdová, M., Rohovec, J., Chrastný, V., Penížek, V., and Navrátil, T.: The influence of sample drying procedures on
613 mercury concentrations analyzed in soils, Bulletin of environmental contamination and toxicology, 94, 570–
614 576, doi:10.1007/s00128-015-1521-9, 2015.
615 Horvat, M., Nolde, N., Fajon, V., Jereb, V., Logar, M., Lojen, S., Jacimovic, R., Falnoga, I., Liya, Q., Faganeli, J.,
616 and Drobne, D.: Total mercury, methylmercury and selenium in mercury polluted areas in the province Gui-
617 zhou, China, Science of The Total Environment, 304, 231–256, doi:10.1016/S0048-9697(02)00572-7, 2003.
618 Hu, H., Li, M., Wang, G., Drosos, M., Li, Z., Hu, Z., and Xi, B.: Water-soluble mercury induced by organic
619 amendments affected microbial community assemblage in mercury-polluted paddy soil, Chemosphere, 236,
620 124405, doi:10.1016/j.chemosphere.2019.124405, 2019.
621 Jiskra, M., Wiederhold, J. G., Skyllberg, U., Kronberg, R.-M., and Kretzschmar, R.: Source tracing of natural organ-
622 ic matter bound mercury in boreal forest runoff with mercury stable isotopes, Environmental science. Processes
623 & impacts, 19, 1235–1248, doi:10.1039/c7em00245a, 2017.
624 Jones, M. E., Nico, P. S., Ying, S., Regier, T., Thieme, J., and Keiluweit, M.: Manganese-Driven Carbon Oxidation
625 at Oxic-Anoxic Interfaces, Environmental science & technology, 52, 12349–12357,
626 doi:10.1021/acs.est.8b03791, 2018.
627 Jonsson, S., Skyllberg, U., Nilsson, M. B., Westlund, P.-O., Shchukarev, A., Lundberg, E., and Björn, E.: Mercury
628 methylation rates for geochemically relevant Hg(II) species in sediments, Environmental science & technology,
629 46, 11653–11659, doi:10.1021/es3015327, 2012.

https://doi.org/10.5194/bg-2020-466
Preprint. Discussion started: 1 February 2021

630 Kronberg, R.-M., Jiskra, M., Wiederhold, J. G., Björn, E., and Skyllberg, U.: Methyl Mercury Formation in
631 Hillslope Soils of Boreal Forests: The Role of Forest Harvest and Anaerobic Microbes, Environmental science
632 & technology, 50, 9177–9186, doi:10.1021/acs.est.6b00762, 2016.
633 Li, H., Zheng, D., Zhang, X., Niu, Z., Ma, H., Zhang, S., and Wu, C.: Total and Methylmercury of Suaeda heterop-
634 tera Wetland Soil Response to a Salinity Gradient Under Wetting and Drying Conditions, Bulletin of environ-
635 mental contamination and toxicology, 104, 778–785, doi:10.1007/s00128-020-02874-1, 2020.
636 Liang, X., Lu, X., Zhao, J., Liang, L., Zeng, E. Y., and Gu, B.: Stepwise Reduction Approach Reveals Mercury
637 Competitive Binding and Exchange Reactions within Natural Organic Matter and Mixed Organic Ligands, En-
638 vironmental science & technology, 53, 10685–10694, doi:10.1021/acs.est.9b02586, 2019.
639 Liu, Y.-R., Dong, J.-X., Han, L.-L., Zheng, Y.-M., and He, J.-Z.: Influence of rice straw amendment on mercury
640 methylation and nitrification in paddy soils, Environmental pollution (Barking, Essex 1987), 209, 53–59,
641 doi:10.1016/j.envpol.2015.11.023, 2016.
642 Ma, D., Wu, J., Yang, P., and Zhu, M.: Coupled Manganese Redox Cycling and Organic Carbon Degradation on
643 Mineral Surfaces, Environmental science & technology, doi:10.1021/acs.est.0c02065, 2020.
644 Manceau, A., Lemouchi, C., Enescu, M., Gaillot, A.-C., Lanson, M., Magnin, V., Glatzel, P., Poulin, B. A., Ryan, J.
645 N., Aiken, G. R., Gautier-Luneau, I., and Nagy, K. L.: Formation of Mercury Sulfide from Hg(II)-Thiolate
646 Complexes in Natural Organic Matter, Environmental science & technology, 49, 9787–9796,
647 doi:10.1021/acs.est.5b02522, 2015.
648 Manceau, A., Nagy, K. L., Marcus, M. A., Lanson, M., Geoffroy, N., Jacquet, T., and Kirpichtchikova, T.: For-
649 mation of metallic copper nanoparticles at the soil-root interface, Environmental science & technology, 42,
650 1766–1772, doi:10.1021/es072017o, 2008.
651 Marvin-DiPasquale, M., Windham-Myers, L., Agee, J. L., Kakouros, E., Le Kieu, H., Fleck, J. A., Alpers, C. N.,
652 and Stricker, C. A.: Methylmercury production in sediment from agricultural and non-agricultural wetlands in
653 the Yolo Bypass, California, USA, The Science of the total environment, 484, 288–299,
654 doi:10.1016/j.scitotenv.2013.09.098, 2014.
655 Miller, C. L., Mason, R. P., Gilmour, C. C., and Heyes, A.: Influence of dissolved organic matter on the complexa-
656 tion of Hg under sulfidic conditions., Environmental Toxicology and Chemistry, 26, 624–633, 2007.
657 Miller, C. L., Southworth, G., Brooks, S., Liang, L., and Gu, B.: Kinetic controls on the complexation between mer-
658 cury and dissolved organic matter in a contaminated environment, Environmental science & technology, 43,
659 8548–8553, doi:10.1021/es901891t, 2009.
660 Neculita, C.-M., Zagury, G. J., and Deschênes, L.: Mercury speciation in highly contaminated soils from chlor-alkali
661 plants using chemical extractions, Journal of environmental quality, 34, 255–262, 2005.
662 Ponting, J., Kelly, T. J., Verhoef, A., Watts, M. J., and Sizmur, T.: The impact of increased flooding occurrence on
663 the mobility of potentially toxic elements in floodplain soil - A review, The Science of the total environment,
664 754, 142040, doi:10.1016/j.scitotenv.2020.142040, 2020.

https://doi.org/10.5194/bg-2020-466
Preprint. Discussion started: 1 February 2021

665 Poulin, B. A., Aiken, G. R., Nagy, K. L., Manceau, A., Krabbenhoft, D. P., and Ryan, J. N.: Mercury transformation
666 and release differs with depth and time in a contaminated riparian soil during simulated flooding, Geochimica et
667 Cosmochimica Acta, 176, 118–138, doi:10.1016/j.gca.2015.12.024, 2016.
668 Qiu, G., Feng, X., Wang, S., and Shang, L.: Mercury and methylmercury in riparian soil, sediments, mine-waste
669 calcines, and moss from abandoned Hg mines in east Guizhou province, southwestern China, Applied Geo-
670 chemistry, 20, 627–638, doi:10.1016/j.apgeochem.2004.09.006, 2005.
671 Ravichandran, M.: Interactions between mercury and dissolved organic matter--a review, Chemosphere, 55, 319–
672 331, doi:10.1016/j.chemosphere.2003.11.011, 2004.
673 Ravichandran, M., Aiken, G. R., Ryan, J. N., and Reddy, M. M.: Inhibition of Precipitation and Aggregation of
674 Metacinnabar (Mercuric Sulfide) by Dissolved Organic Matter Isolated from the Florida Everglades, Environ.
675 Sci. Technol., 33, 1418–1423, doi:10.1021/es9811187, 1999.
676 Richner, W. and Sinaj, S.: Grundlagen für die Düngung landwirtschafltlicher Kulturen in der Schweiz (GRUD 2017),
677 Agroscope, Bern, Schweiz, 276 pp., 2017.
678 Rivera, N. A., Bippus, P. M., and Hsu-Kim, H.: Relative Reactivity and Bioavailability of Mercury Sorbed to or
679 Coprecipitated with Aged Iron Sulfides, Environmental science & technology, 53, 7391–7399,
680 doi:10.1021/acs.est.9b00768, 2019.
681 Siemens, J. and Kaupenjohann, M.: Dissolved organic carbon is released from sealings and glues of pore-water
682 samplers, Soil Science Society of America Journal, 67, 795–797, 2003.
683 Singer, M. B., Harrison, L. R., Donovan, P. M., Blum, J. D., and Marvin-DiPasquale, M.: Hydrologic indicators of
684 hot spots and hot moments of mercury methylation potential along river corridors, The Science of the total envi-
685 ronment, 568, 697–711, doi:10.1016/j.scitotenv.2016.03.005, 2016.
686 Skyllberg, U.: Competition among thiols and inorganic sulfides and polysulfides for Hg and MeHg in wetland soils
687 and sediments under suboxic conditions: Illumination of controversies and implications for MeHg net produc-
688 tion, J. Geophys. Res., 113, n/a-n/a, doi:10.1029/2008JG000745, 2008.
689 Skyllberg, U., Bloom, P. R., Qian, J., Lin, C.-M., and Bleam, W. F.: Complexation of mercury(II) in soil organic
690 matter: EXAFS evidence for linear two-coordination with reduced sulfur groups, Environmental science &
691 technology, 40, 4174–4180, doi:10.1021/es0600577, 2006.
692 Skyllberg, U. and Drott, A.: Competition between disordered iron sulfide and natural organic matter associated
693 thiols for mercury(II)-an EXAFS study, Environmental science & technology, 44, 1254–1259,
694 doi:10.1021/es902091w, 2010.
695 Sunda, W. G. and Kieber, D. J.: Oxidation of humic substances by manganese oxides yields low-molecular-weight
696 organic substrates, Nature, 367, 62-64, 1994.
697 Tang, W., Hintelmann, H., Gu, B., Feng, X., Liu, Y., Gao, Y., Zhao, J., Zhu, H., Lei, P., and Zhong, H.: Increased
698 Methylmercury Accumulation in Rice after Straw Amendment, Environmental science & technology, 53, 6144–
699 6153, doi:10.1021/acs.est.8b07145, 2019.

https://doi.org/10.5194/bg-2020-466
Preprint. Discussion started: 1 February 2021

700 Tang, Z., Fan, F., Wang, X., Shi, X., Deng, S., and Wang, D.: Mercury in rice (Oryza sativa L.) and rice-paddy soils
701 under long-term fertilizer and organic amendment, Ecotoxicology and environmental safety, 150, 116–122,
702 doi:10.1016/j.ecoenv.2017.12.021, 2018.
703 Vlassopoulos, D., Kanematsu, M., Henry, E. A., Goin, J., Leven, A., Glaser, D., Brown, S. S., and O'Day, P. A.:
704 Manganese(iv) oxide amendments reduce methylmercury concentrations in sediment porewater, Environmental
705 science. Processes & impacts, 20, 1746–1760, doi:10.1039/c7em00583k, 2018.
706 Wang, Y., Chen, Z., Wu, Y., and Zhong, H.: Comparison of methylmercury accumulation in wheat and rice grown
707 in straw-amended paddy soil, The Science of the total environment, 697, 134143,
708 doi:10.1016/j.scitotenv.2019.134143, 2019.
709 Wang, Y., Dang, F., Zhong, H., Wei, Z., and Li, P.: Effects of sulfate and selenite on mercury methylation in a mer-
710 cury-contaminated rice paddy soil under anoxic conditions, Environmental science and pollution research inter-
711 national, 23, 4602–4608, doi:10.1007/s11356-015-5696-8, 2016.
712 Weber, F.-A., Voegelin, A., Kaegi, R., and Kretzschmar, R.: Contaminant mobilization by metallic copper and metal
713 sulphide colloids in flooded soil, Nature Geoscience, 2, 267–271, doi:10.1038/ngeo476, 2009.
714 Zhang, T., Kim, B., Levard, C., Reinsch, B. C., Lowry, G. V., Deshusses, M. A., and Hsu-Kim, H.: Methylation of
715 mercury by bacteria exposed to dissolved, nanoparticulate, and microparticulate mercuric sulfides, Environmen-
716 tal science & technology, 46, 6950–6958, doi:10.1021/es203181m, 2012.
717 Zhang, Y., Liu, Y.-R., Lei, P., Wang, Y.-J., and Zhong, H.: Biochar and nitrate reduce risk of methylmercury in soils
718 under straw amendment, The Science of the total environment, 619-620, 384–390,
719 doi:10.1016/j.scitotenv.2017.11.106, 2018.
720 Zhao, J.-Y., Ye, Z.-H., and Zhong, H.: Rice root exudates affect microbial methylmercury production in paddy soils,
721 Environmental pollution (Barking, Essex 1987), 242, 1921–1929, doi:10.1016/j.envpol.2018.07.072, 2018.
722 Zhu, H., Zhong, H., and Wu, J.: Incorporating rice residues into paddy soils affects methylmercury accumulation in
723 rice, Chemosphere, 152, 259–264, doi:10.1016/j.chemosphere.2016.02.095, 2016.
724

https://doi.org/10.5194/bg-2020-466
Preprint. Discussion started: 1 February 2021

Biogeosciences Discussions Open Access EGU

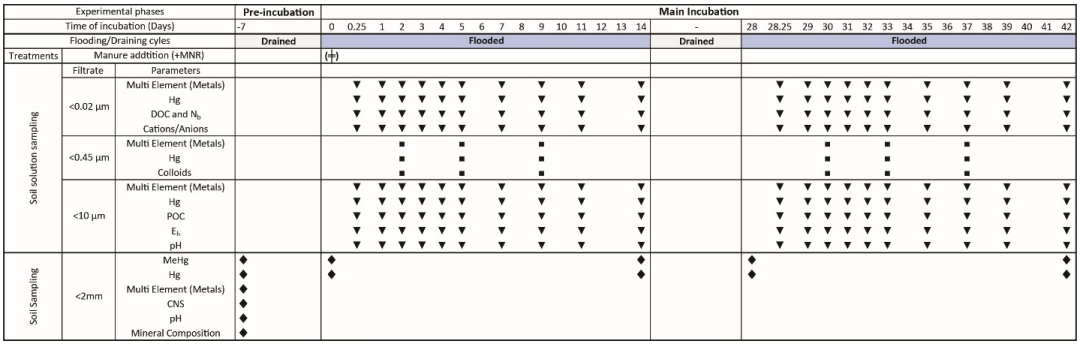

Figure 1: Schedule of performed incubation experiment, samplings and measurements. Blue bars indicate soil flooding periods. Grey bars represent drained periods. The width of the columns is not proportional to the time of incubation. In the treatments row the (⧺) symbol indicates the addition of liquid manure to the microcosms specifically treated with manure (+MNR). Triangles represent regular soil solution sampling points. Rectangles represent soil solution sampling for colloid analyses. Diamonds represent time points for soil sampling. At - 7 days, soil was sampled from the pooled soil directly before the pre-incubation.

https://doi.org/10.5194/bg-2020-466
Preprint. Discussion started: 1 February 2021

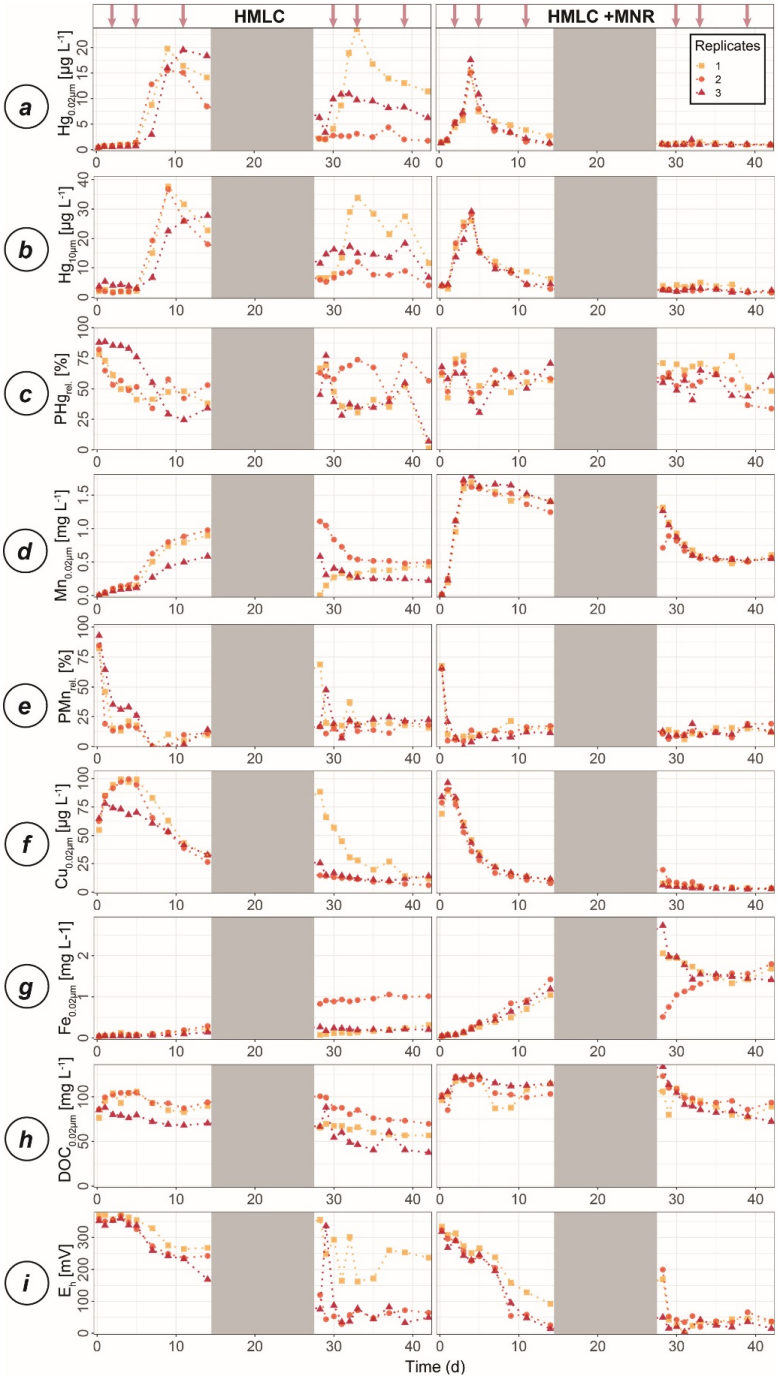

Figure 2: Concentrations of Hg (a-c) and relevant parameters (Mn, PMn, Fe, DOC, Cu, E_h) (d-i) in the soil solution of the cornfield soil (HMLC) incubations. Lines between points were plotted to improve readability. The grey area indicates the drained period. Red arrows indicate sampling days for AF4-ICP-MS analyses.

735

https://doi.org/10.5194/bg-2020-466
Preprint. Discussion started: 1 February 2021

736

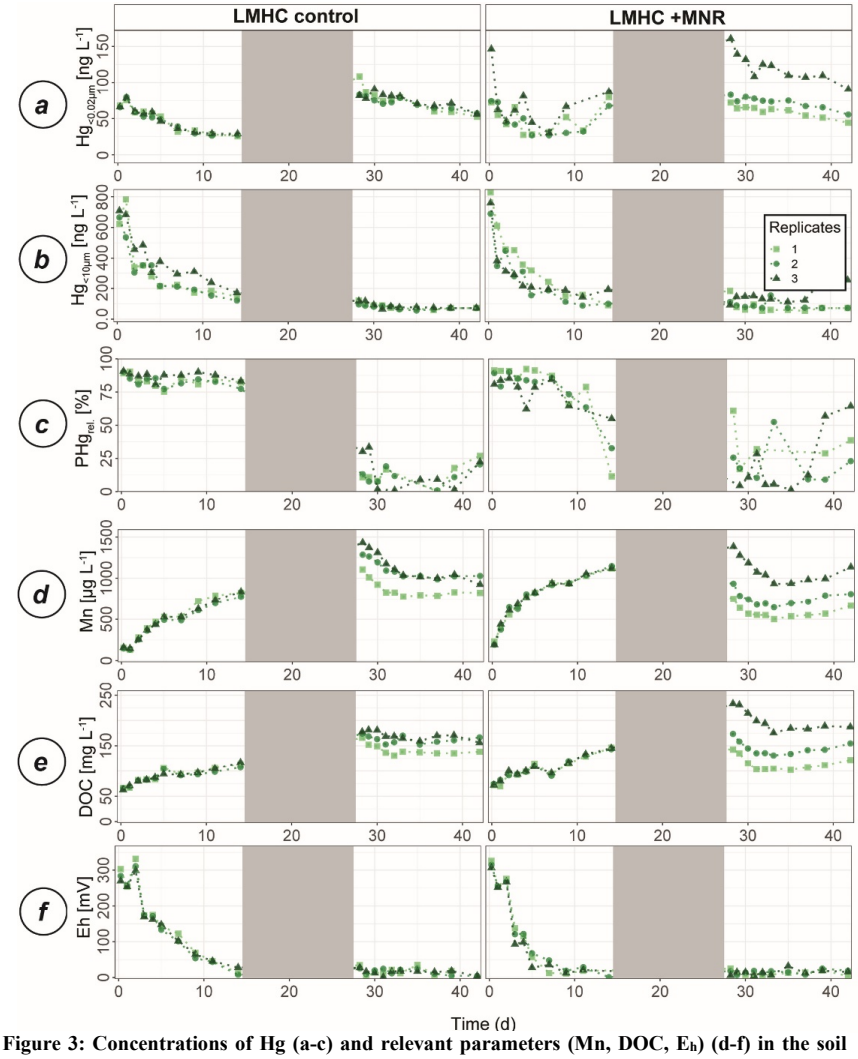

Figure 3: Concentrations of Hg (a-c) and relevant parameters (Mn, DOC, E_h) (d-f) in the soil solution of the pasture field soil (LMHC) incubations. Lines between points were plotted to improve readability. The gray area indicates the drained period. The three shades of green distinguish the 3 replicate incubators.

737

738

739

https://doi.org/10.5194/bg-2020-466
Preprint. Discussion started: 1 February 2021

Biogeosciences Discussions Open Access EGU

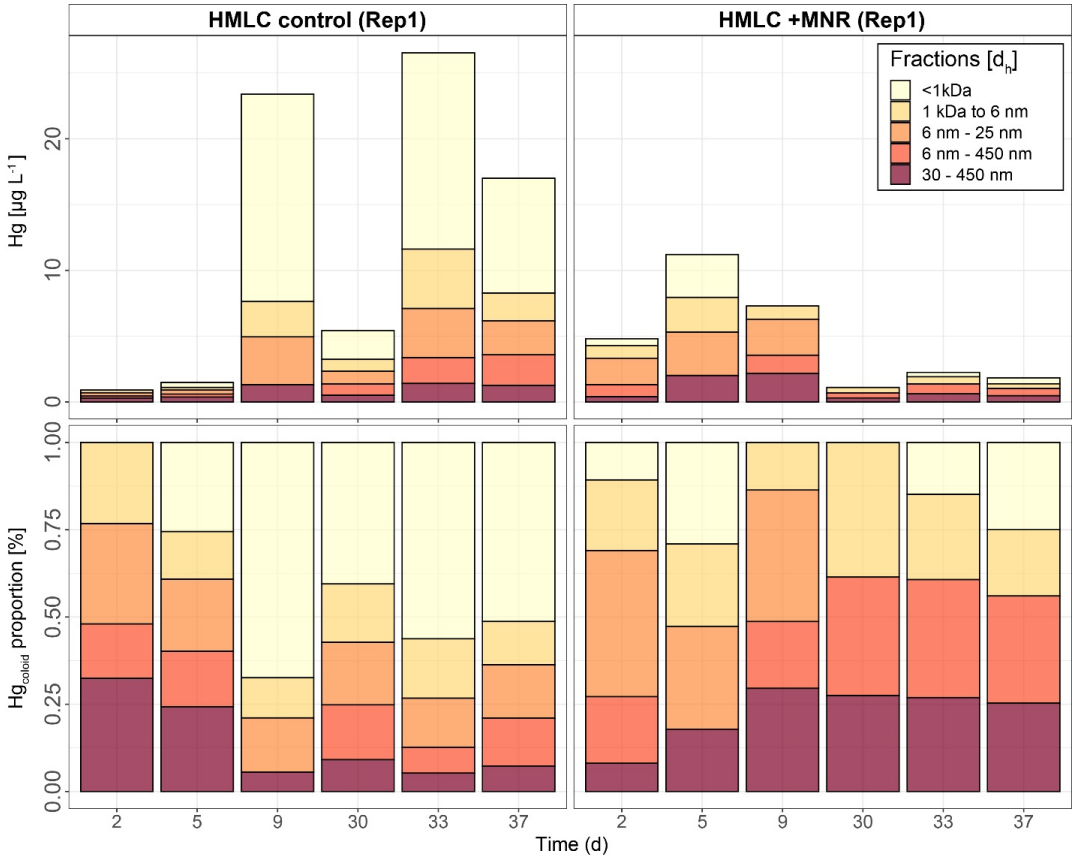

Figure 4: Size distribution of Hg estimated after AF4 fractogram deconvolution for Rep1 of cornfield soil incubation (HMLC and HMLC +MNR). Details on the deconvolution procedure are provided in the supplement. The concentration of Hg in size fractions was calculated using an external calibration of the ICP–MS directly after the AF4 run. The concentration of Hg in "< 1kDa" was calculated by subtracting the sum of the fractions from the total Hg concentration in the sample measured separately by ICP–MS.

740

https://doi.org/10.5194/bg-2020-466
Preprint. Discussion started: 1 February 2021

742

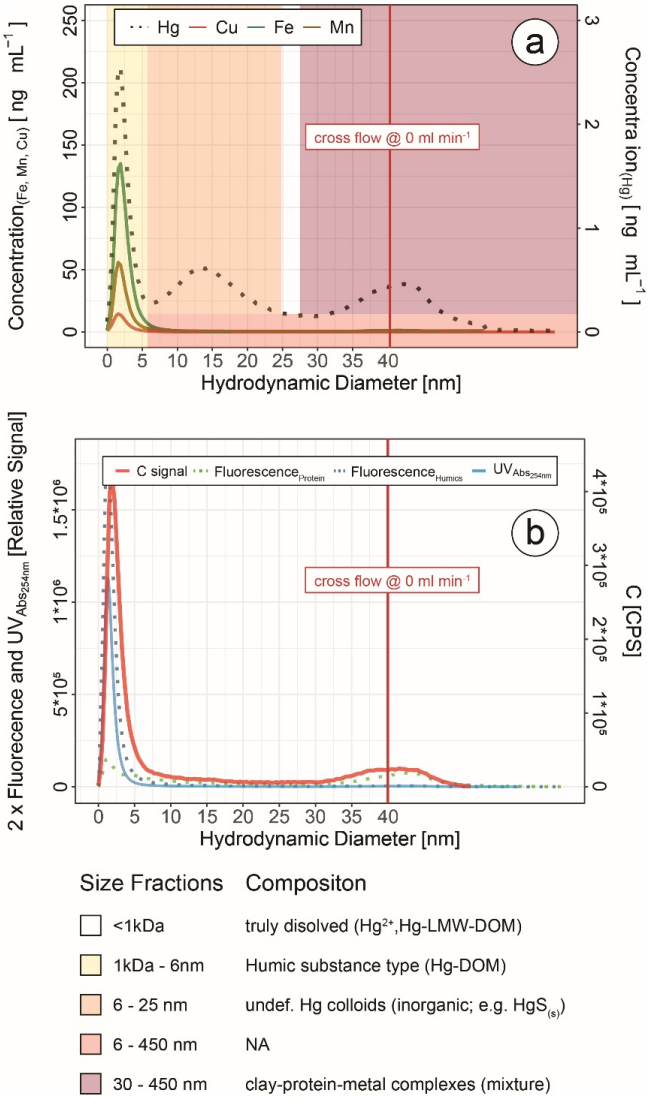

Figure 5: Hg, Cu, Mn and Fe concentrations (a) and C signals (ICP–MS), UV_{254nm} absorbance and fluorescence signals (b) in colloids as a function of hydrodynamic diameter (related to retention times on AF4) in a sample from HMLC at day 9 after flooding. These fractograms were obtained at linearly decreasing crossflow from 2 to 0 mL min^{-1} over 20 min. The red line indicates the time point where the crossflow reached 0 ml min^{-1}. Areas (yellow to red color) indicate size fraction ranges assigned during deconvolution.

https://doi.org/10.5194/bg-2020-466
Preprint. Discussion started: 1 February 2021

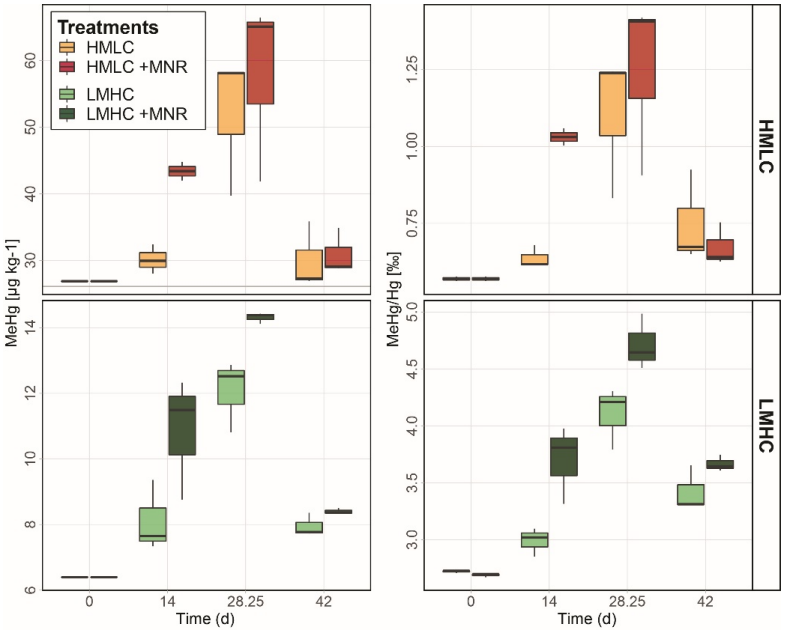

743

744 **Figure 6: Soil MeHg concentrations and MeHg/Hg ratios over the course of the experi-**
745 **ment for corn field soils (HMLC, red) and pasture field soils (LMHC, green). Highest**
746 **net methylation was observed during first flooding (for +MNR treatments) and during**
747 **the draining period (control). A significant decrease of MeHg/Hg was observed during**
748 **the second flooding for all treatments.**

749

750

https://doi.org/10.5194/bg-2020-466
Preprint. Discussion started: 1 February 2021

751 **Table 1: Description of the symbols and terms used for different filter fractions in the publication. The particulate frac-**
752 **tion is calculated as the difference of the 20 nm and the 10µm filtrate concentrations.**

Filter Type	Filter size	Symbol (e.g. Hg_x)	Description
Suction Cup	10 µm	$Hg_{<10µm}$	Soil solution sampled directly from the suction cup contains a variety of particles (clay minerals, bacteria, Mn-/Fe-hydroxides, POM aggregates etc.). We refer to this fraction by adding the suffix <10µm to the analyte symbol.
Syringe Filter	0.02 µm	$Hg_{<0.02µm}$	Soil solution <0.02µm is a cutoff size that may still carry colloids. We refer to this fraction by adding the suffix <0.02µm to the analyte symbol.
-	-	PHg	Particulate Hg is calculated as: $PHg = Hg_{<10µm} - Hg_{<0.02µm}$
-	-	$PHg_{rel.}$	Particulate Hg is calculated as: $PHg_{rel.} = (Hg_{<10µm} - Hg_{<0.02µm})/Hg_{<10µm}$
AF4 membrane	1 kDa	$Hg_{<1kDa}$	Molecules in solution under this cutoff size are not expected to have colloidal properties. Therefore, this range is referred to as "truly dissolved" in the text.

753

https://doi.org/10.5194/bg-2020-466
Preprint. Discussion started: 1 February 2021

754 **Table 2: List of soil parameters for the two incubated soils (HMLC and LMHC) and manure (MNR)**

Parameter		Cornfield (HMLC)		Pasture field (LMHC)		Cow Manure (MNR)	
Land use		Corn field		Pasture		-	
Depth		0 - 20 cm		0 - 20 cm		-	
Soil Type (WRB)		Fluvisol Gleyic		Fluvisol Gleyic		-	
pH_{CaCl2}		8.16		7.84		-	
Water content	(wt. %)	13.8		8.5		90.3	
	Unit (dry.wt.)	Concentration	SD	Concentration	SD	Concentration	SD
C_{org}	wt. %	1.92	0.01	3.45	0.01	45.22	0.09
N_{tot}	wt. %	0.181	0.001	0.372	0.002	3.68	0.08
C_{org}/N_{tot}	-	10.61	-	9.29	-	-	-
S	g kg^{-1}	0.63	0.05	0.77	0.05	3.7	0.1
Hg	mg kg^{-1}	47.3	0.5	2.4	0.3	0.045	0.001
MeHg	µg/kg	26.9	0.2	6.4	0.2	<0.02	-
MeHg/Hg	%	0.06	-	0.28	-	-	-
Al	wt. %	0.91	0.05	1.05	0.04	0.0106	0.0003
Fe		1.95	0.07	2.38	0.05	0.0336	0.0009
Mg		1.25	0.07	1.39	0.05	0.49	0.03
Mn	mg kg^{-1}	493	21	672	38	53	1
P		1169	80	1044	85	8245	232
Cr		56	4	64	5	0.68	0.01
Co		10.75	0.06	11.22	0.43	0.4	0.2
Ni		81.7	0.8	78.3	2.9	2.3	0.1
Cu		40.1	1.2	28.0	0.7	13.1	0.6
Zn		61.8	0.5	47.3	2.0	81	3
As		11.74	0.07	16.04	0.72	0.8	0.4
Cd		0.21	0.04	0.17	0.01	0.042	0.004
Pb		20.8	0.5	18.34	0.5	-	-
V		17.2	0.4	20.99	1.1	0.31	0.01
Sr		137	2	202	6	45.9	1.6
Cs		1.99	0.02	1.52	0.04	-	-
Ba		60.2	1.1	76.9	1.6	9.1	0.5
Ce		7.0	0.4	8.6	0.6	-	-
Gd		0.94	0.03	1.00	0.05	0.021	0.001
U		1.74	0.08	1.29	0.01	0.19	0.01
Hg/Cu molar	‰	366.3	-	25.73	-	-	-
Hg/Mn molar		25.758	-	0.926	-	-	-
Hg/C_{org} molar		0.147	-	0.004	-	-	-
Mn/C_{org} molar		0.0056	-	0.0042	-	-	-

755

756

757

https://doi.org/10.5194/bg-2020-466
Preprint. Discussion started: 1 February 2021

758

759 **Table 3: Soil MeHg concentrations and net-methylation (MeHg/Hg) over the time of the experiment.**

Treatment	day	n	Mean MeHg (µg kg^{-1})	SD MeHg (µg kg^{-1})	Range MeHg (µg kg^{-1})	MeHg/Hg (‰)	de-/methylation (%)
HMLC	0	1	26.9	-	26.9 - 26.9	0.57	-
	14	3	30.14	2.19	28.04 - 32.42	0.64	12.0
	28	3	52.04	10.65	39.74 - 58.25	1.1	73.1
	42	3	30.03	5.05	26.93 - 35.86	0.75	-32.4
HMLC +MNR	0	1	26.9	-	26.9 - 26.9	0.57	-
	14	3	43.41	1.99	42 - 44.81	1.03	81.1
	28	3	57.79	13.79	41.88 - 66.41	1.24	20.7
	42	3	30.94	3.43	28.85 - 34.9	0.67	-45.9
LMHC	0	1	6.4	-	6.4 - 6.4	2.72	-
	14	3	8.11	1.09	7.33 - 9.36	2.99	10.0
	28	3	12.07	1.1	10.81 - 12.87	4.11	37.2
	42	3	7.95	0.35	7.73 - 8.36	3.42	-16.7
LMHC +MNR	0	1	6.4	-	6.4 - 6.4	2.69	-
	14	3	10.86	1.86	8.76 - 12.32	3.72	38.1
	28	3	14.31	0.17	14.12 - 14.43	4.7	26.6
	42	3	8.4	0.09	8.33 - 8.5	3.67	-22.0

760

761